Versatile element for free-space dividing and redirecting neutral atom clouds

I. V. Arakelyan,[1] N. Chattrapiban[1], S. Mitra[2] and W. T. Hill, III[1,2]
[1]*Department of Physics and*
[2]*Institute for Physical Science and Technology University of Maryland, College Park, Maryland 20742, USA**
(Dated: November 28, 2005)

We introduce a *tunnel lock* that can be exploited to divide, delay and alter the direction of traveling clouds of cold atoms. This versatile free-space element is implemented by crossing two atom tunnels formed by low intensity, blue-detuned dark-hollow (Bessel mode) laser beams. We show that clouds of cold ^{87}Rb atoms initially moving within one tunnel can be transferred to the other by gating the intensities of the two tunnels – a tunnel lock – with an efficiency limited by the overlap volume. The element also can be used to divide a single cloud into smaller clouds each having a distinct momentum.

PACS numbers:

Controlling the external degrees of freedom of ensembles of neutral atoms is key to realizing a host of future applications from atom interferometry to quantum computing. Achieving durable control requires robust atom optical elements (1) to move ensembles along arbitrary paths and (2) to divide, delay, recombine and reshape ensembles at any location along the path, in the absence of decoherence. A number of different techniques for switching and dividing neutral atom clouds have been proposed and demonstrated over the past few years. Exploiting atomic magnetic moments, for example, guides and switches have been produced with magnetic fields from current carrying wires [1]; circuits have been fabricated on surfaces (atom chips) [2, 3]. More recently, chip-based interferometers have been demonstrated where Bose-Einstein condensates have been split with an optical grating (via diffraction) [4] and double-welled magnetic potentials [5].

Light-based techniques have been used as well to divide clouds of atoms in free-space. Free-space elements have attractive features not easily realized with contemporary material-based element designs making them potentially versatile compliments to the atom optical element arsenal. Atomic magnetic moments, for example, are not required. More importantly, light-based elements can be formed anywhere in space and modified in real-time, making them compatible with a variety of cold atom sources. Simple elements have been reported with red-detuned TEM_{00} modes [6] as have more sophisticated interferometer structures [7]. The development of elements built upon hollow (donut-type) laser modes [8, 9] would be particularly useful for a variety of reasons. Specifically, they can be produced via mode conversion with two-dimensional programmable spatial light modulators (SLM) [10, 11] with relatively low intensity (< 1 W) cw laser beams tuned only a few gigahertz to the blue of an atomic resonance. A reasonable scattering rate is maintained because the atoms spend most of their time in the dark [8]. Far-blue detuned operation would essentially eliminate absorption and would be possible at condensate temperatures with high power Ar^+ laser. At high intensities, hollow beams can be generated with axicons, for example [8]. Near resonance operation, suitable for MOT temperature atoms, means the same lasers used to trap the atoms can be used to generate the elements. Detuning can be used, in this case, as a knob to accelerate or slow the ensemble [8]. Finally, as we show in this paper, delay lines and beam dividers can be realized by crossing two hollow tunnels.

While free-space neutral atom beam dividers based on crossing two red-detuned TEM_{00} (filled) tunnels have been demonstrated [6], similar elements have not been reported for blue-detuned hollow tunnels. This is due in part to the fact that transferring atoms between two crossed blue-detuned hollow tunnels cannot be done passively; a modulation of both tunnel intensities is required. The modulation – gating the intensities on and off – produces a *tunnel lock*, where the barrier caused by the intensity of the second or crossed tunnel is momentarily lowered (entrance gate opened) to allow the cloud to be positioned in both tunnels simultaneously. When the intensity of the second tunnel is raised (entrance gate closed), a portion of the cloud will be trapped in three dimensions. When the intensity of the first tunnel is reduced (exit gate opened), the confined portion of the cloud will be free to travel within the second tunnel with a different momentum (i.e., with a different direction and perhaps speed). These gates are illustrated in Fig. 1. As we will show, we can create beam dividers, delay lines and switches with an appropriate timing of the gates.

The purpose of this paper is to present a prototype version of the *tunnel lock* that we used (1) to change the momentum of a traveling cloud and (2) to divide one cloud into three distinct clouds. Our demonstration was performed with 10^8 Rb atoms collected from a vapor background of $\sim 10^{-8}$ Torr into a magneto-optical

Report Documentation Page

Form Approved
OMB No. 0704-0188

1. REPORT DATE **28 NOV 2005**	2. REPORT TYPE	3. DATES COVERED **00-00-2005 to 00-00-2005**
4. TITLE AND SUBTITLE **Versatile element for free-space dividing and redirecting neutral atom clouds**		5a. CONTRACT NUMBER 5b. GRANT NUMBER 5c. PROGRAM ELEMENT NUMBER
6. AUTHOR(S)		5d. PROJECT NUMBER 5e. TASK NUMBER 5f. WORK UNIT NUMBER
7. PERFORMING ORGANIZATION NAME(S) AND ADDRESS(ES) **University of Maryland,8400 Baltimore Avenue,College Park,MD,20742**		8. PERFORMING ORGANIZATION REPORT NUMBER
9. SPONSORING/MONITORING AGENCY NAME(S) AND ADDRESS(ES)		10. SPONSOR/MONITOR’S ACRONYM(S) 11. SPONSOR/MONITOR’S REPORT NUMBER(S)
12. DISTRIBUTION/AVAILABILITY STATEMENT **Approved for public release; distribution unlimited**		
13. SUPPLEMENTARY NOTES		
14. ABSTRACT		
15. SUBJECT TERMS		

16. SECURITY CLASSIFICATION OF:			17. LIMITATION OF ABSTRACT	18. NUMBER OF PAGES	19a. NAME OF RESPONSIBLE PERSON
a. REPORT **unclassified**	b. ABSTRACT **unclassified**	c. THIS PAGE **unclassified**		**4**	

Standard Form 298 (Rev. 8-98)
Prescribed by ANSI Std Z39-18

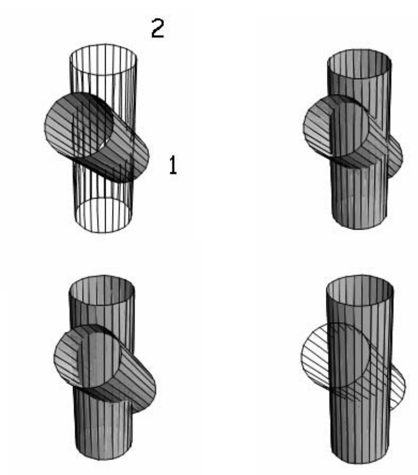

FIG. 1: Schematic of the tunnel lock with perfect beam overlap at the cross point, upper row and right column and partial overlap, lower left. The solid (wire-frame) cylinders represent the tunnel being on (off). Gate status, counterclockwise from upper left: entrance (exit) gate open (closed), entrance (exit) gate closed (closed), entrance (exit) gate closed (open) and entrance (exit) gate closed (closed).

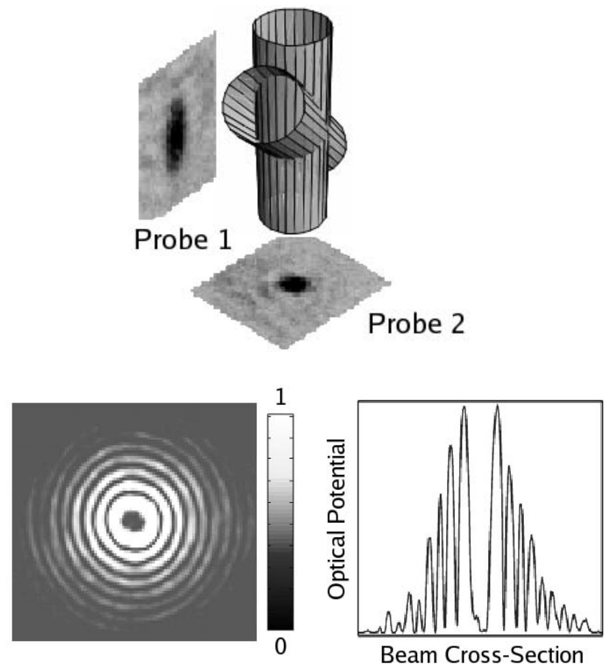

FIG. 2: Schematic of the imaging arrangement where the tunnels cross with probe 1 (2) monitoring traveling clouds in tunnel 2 perpendicular (parallel) to the direction of propagation. The lower left image is a typical contour of the transverse intensity profile of a J_4 mode tunnel of diameter 1 mm. The lower right figure is the corresponding radial dependence of the optical potential due to the dipole force.

trap (MOT) held at $\sim$ 250 μK with a cloud diameter of 1.0 - 1.5 mm. The tunnel lock and associated elements were generate with two hollow mode laser beams directed vertically and crossed at an angle of $\sim 12^\circ$ at the MOT cloud. The hollow modes had intensity profiles $\propto \mathrm{J}^2_{n=4}(kr)$ [10]. Bessel modes, which are solutions to the wave equation known to propagate nearly diffraction free [12], have zero intensity along their propagation axis for all modes with $n \geq 1$. The first ring of the $n \neq 0$ modes forms a hollow thin-walled cylinder of light (see Fig. 2) in which the atoms can be trapped in the transverse direction but free to move longitudinally [11]. The force containing the atoms is generated by the interaction between the electric field gradient of the light and the induced dipole moment of an atom. All experiments were carried out at a detuning of +4 GHz, tunnel diameters (measured as a peak-to-peak diameter of the first light ring of the Bessel mode) of $\sim$ 1 mm and 80 mW of power in the first ring. At this detuning the potential height was $\sim$ 250 μK. The photon scattering rate was estimated to be ~ 2000 s^{-1} leading to an average heating rate of $\lesssim 1$ μK/ms, < 20 μK over the length of each experiment.

A single SLM converted 500 mW of a TEM_{00} mode from a Ti:sapphire laser into a single Bessel mode beam[11]. This was followed by an optical beam splitter to divide the Bessel-mode beam into two tunnels. The traveling atomic cloud was monitored with shadow imaging with two probe beams tuned to the Rb resonant transition both perpendicular and parallel to the tunnels as shown in Fig. 2.

As mentioned above, the prototype tunnel lock was used to divide and to switch the direction of a moving ensemble of cold atoms. To demonstrate the switch, where the path of a moving cloud was deviated, a portion of the MOT cloud was launched into tunnel 1 by turning off the MOT laser beams. The relative intensities of the MOT laser beams were adjusted to give the MOT cloud an initial boost of $\sim$ 1.5 mm/ms along tunnel 1. Figure 3 shows a 12 ms sequence of images of the cloud obtained with probes 1 and 2. Only one tunnel was on when these images were captured. There are several features to be noted about these images. First, only a portion of the MOT atoms are confined to the tunnels; it takes $\sim$ 10 ms before the confined atoms can be distinguished from those not confined. From probe 1, the cloud assumes a long oval shape when confined (see also Fig. 2). The cloud elongates from $\sim$ 1.5 mm to $\sim$ 2.5 mm during the first 10 ms and drops $\sim$ 2 mm. From probe 2, the cloud confined to tunnel 2 takes on a circular shape (see Fig. 2) and a stubby oval shape when confined to tunnel 1. These shapes can be understood from the schematic in Fig. 2. Probe 2 was used to confirm confinement for at least 20 ms; the integrated column density along the tunnel (NL) was nearly constant between 10 and 20 ms.

We deviated the direction of a cloud initially traveling

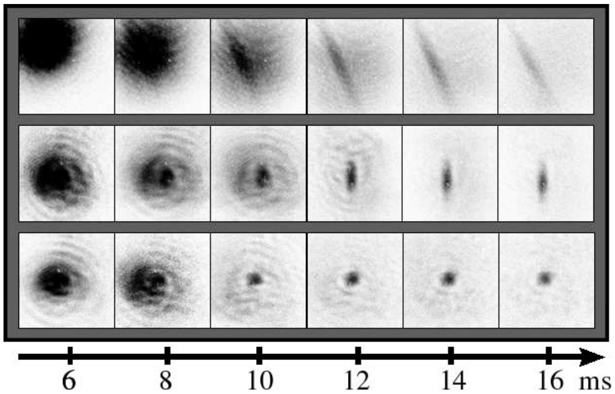

FIG. 3: Shadow images of ^{87}Rb atoms falling under gravity in a single 1 mm diameter tunnel in steps of 2 ms, starting 6 ms after the cloud was launched. The top (two lower) panels correspond to probe 1 (2) of Fig. 2. The middle (bottom) panel corresponds to tunnel 1 (2). Each panel is an average of four frames. First three images of each sequence are saturated, all the images are presented on the same intensity scale.

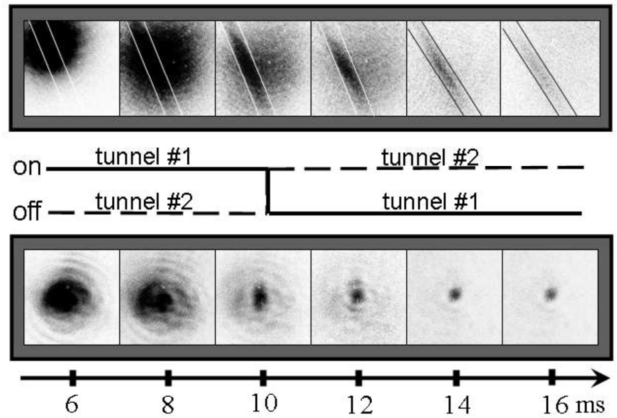

FIG. 4: Shadow images of the cloud of Rb atoms as it passes through the tunnel lock and is switched between tunnels. The upper (lower) series is the evolution of the cloud for 16 ms after it was launched as seen by probe 1 (2). The line graph indicates the state of the tunnels. Each panel is an average of four frames. First three images of each sequence are saturated, all the images are presented on the same intensity scale.

in tunnel 1 by 12° with the following lock operations. At $t = 0$, the cloud was launched in tunnel 1 (MOT laser beams were turned off with a mechanical shutter) and the entrance gate was opened (tunnel 1 on and tunnel 2 off). At $t = 10$ ms, the entrance gate was closed (tunnel 2 on) and the exit gate was opened (tunnel 1 off) simultaneously. The upper (lower) sequence of images in Fig. 4 are the shadows produced by probe 1 (2) following the cloud for 12 ms. The solid lines in the upper sequence indicate the position of tunnel 1 for $t = 6$ to 10 ms and the position of tunnel 2 for $t > 12$ ms. We see that 2 ms after the switch was activated, the 12 ms panel of the upper sequence of images, the cloud is no longer aligned with tunnel 1 (tunnel 1 off and tunnel 2 on at this point). At this stage the cloud is confined by tunnel 2; the remaining panels show the cloud aligning itself with tunnel 2. This redirection of the cloud can be seen more acutely from probe 2 (the lower panels). The switch from tunnel 1 to tunnel 2 is accompanied by the shape change of the cloud from a stubby oval to a circle. Compare the lower sequence of Fig. 4 with the two lower sequences of Fig. 3; recall that Fig. 3 was obtained with tunnel 1 on continuously and tunnel 2 off. At 10 ms, the cloud has the stubby oval shape indicating it was conformed to tunnel 1. The shape changes to that of a circle for the 12 to 16 ms panels, indicating the cloud is propagating in tunnel 2 during this period of time.

We estimate a switch efficiency of ~ 33 % for this demonstration, by comparing NL of the 10 ms frame in Fig. 4, bottom panels (before the redirection was activated) with that at 14 ms, after the redirection is fully completed. During the switch, significant fraction of atoms does not get re-trapped by tunnel 2. Therefore the transient 12 ms frame was disregarded from the analysis to ensure that those atoms do not contribute into the column density (compare 12 and 14 ms panels). The loss rate of tunnel 2 was calculated from the images of bottom panels in Fig. 3, and used to extrapolate NL of the 12 ms frame based on the column density of 14 ms frame in Fig. 4. The reported efficiency is the ratio between the measured NL of the 10 ms panel and extrapolated one at 12 ms. It is clear from Fig. 4 that before the second tunnel was turned on, the cloud extended beyond the intersection volume – the stubby oval is longer than the diameter of the circle. Thus, the measured efficiency is limited in part by the size of the overlap volume. A more accurate determination of the efficiency requires colder atoms and smaller clouds.

The prototype beam divider was created by crossing the two tunnels near the lower portion of the MOT cloud and releasing the cloud with both tunnels on continuously. Figure 5 shows that the MOT cloud overlapped several different volumes at $t = 0$ (before the MOT lasers were extinguished): tunnels 1 and 2 above the cross volume, the cross volume and the volume outside both tunnels. When the MOT is switched off, three distinct clouds with three distinct momenta evolve. Two of these moved freely within the tunnels away from the cross position while the third was trapped within the intersection volume. The atoms trapped between the two tunnels were clearly delayed relative to the other two clouds. Subsequent gating of the tunnel intensities could be used to produce two or more clouds within a tunnel. The bulk of the atoms comprising the traveling clouds below the trap volume in Fig. 5 originate within the tunnels, but slipped by the intersection point. These atoms were not

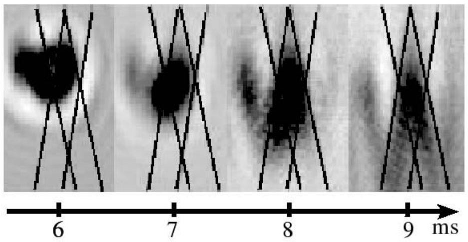

FIG. 5: Beam divider and delay line created with two crossed tunnels (solid lines). Both tunnels were on when the cloud was launched. Three different momentum groups were generated: one moving downward to the left, one moving downward to the right and one stationary relative to the lab frame (i.e., trapped between the two tunnels). Each panel is an average of four frames obtained in the far-field.

trapped because there was only partial overlap between the two tunnels in this demonstration (see the lower left construction in Fig. 1). With better overlap, additional constraints can be placed on the clouds, leading to further possibilities. For example, clouds could be trapped not only within the intersection volume, but above it (in a gravitational field) in one or both tunnels depending on alignment. Multiple bunches of clouds traveling within a tunnel with selectable delays could be created by gating the tunnels intensities in much the same way already discussed.

It is clear from Figs. 4 and 5 that hollow laser beams, with proper timing of the tunnel lock, can be exploited to create four essential elements for free-space atom interferometry – guides or tunnels, dividers, switches and delays. While the atoms used in the demonstration were obtained from a relatively warm source of atoms (average ensemble temperature was a significant fraction of the potential height) the elements will function more efficiently with a colder source of atoms and more compact clouds. Colder atoms would allow larger detunings to be used reducing the heating rate. Absorption can be virtually eliminated with far-blue detuning using Ar^+ lasers, which would be most appropriate for manipulation of Bose-Einstein condensates. Finally, the tunnel locks we have demonstrated can be applied to red-detuned (filled) tunnels as well. Since increasing the intensity essentially deepens the potential well for red-detuned tunnels, it is not clear how to stop a traveling cloud with a diffractionless laser beam (i.e., J_0) that does not come to a focus without introducing additional beams. This is possible with blue-detuned tunnels because blue detuning raises the barrier. Nevertheless, intensity modulation should allow the branching between the two tunnels to be modified with red-detuned Bessel tunnels. At the same time, interferometer structures are easier to envision with red-detuned beams [7]. Consequently, for greater flexibility in free-space manipulation of neutral ensembles, elements based on both red and blue detuning will be required.

We would like to thank Drs. M. Coplan and A. Goussev for extensive discussions and a number of valuable comments. This work was supported by the U.S. Army Research Office grant No. ARO-DAAD190110695, the National Science Foundation Grant No. PHY0426696 and the National Institute for Standards and Technology grant No. PHY0426696. The spatial light modulator used in this work was provided by the Photonics Technology Access Program that is funded by the National Science Foundation and the Defense Advanced Research Projects Agency. Chattrapiban acknowledges support from the Development and Promotion of Science and Technology Talents project of Thailand.

* Electronic address: `wth@ipst.umd.edu`

[1] J. Denschlag, D. Cassettari, A. Chenet, S. Schneider, and J. Schmiedmayer, Appl. Phys. B **69**, 291 (1999).
[2] R. Folman, P. Kruger, D. Cassettari, B. Hessmo, T. Maier, and J. Schmiedmayer, Phys. Rev. Lett. **84**, 4749 (2000).
[3] N. H. Dekker, C. S. Lee, V. Lorent, J. H. Thywissen, S. P. Smith, M. Drndic, R. M. Westervelt, and M. Prentiss, Phys. Rev. Lett. **84**, 1124 (2000).
[4] Y. J. Wang, D. Z. Anderson, V. M. Bright, E. A. Cornell, Q. Diot, T. Kishimoto, M. Prentis, R. A. Saravanan, S. R. Segal, and S. Wu, Phys. Rev. Lett. **94**, 090405 (2005).
[5] Y. Shin, C. Sanner, G. B. Jo, T. A. Pasquini, M. Saba, W. Ketterle, D. E. Pritchard, M. Vengalattore, and M. Prentiss, Phys. Rev. A **72**, 021604 (2005).
[6] O. Houde, D. Kadio, and L. Pruvost, Phys. Rev. Lett. **85**, 5543 (2000).
[7] R. Dumke, T. Müther, M. Volk, W. Ertmer, and G. Birkl, Phys. Rev. Lett. **89**, 220402 (2002).
[8] Y. Song, D. Milam, and W. T. Hill, III, Opt. Lett. **24** (1999).
[9] J. P. Yin, W. J. Gao, and Y. F. Zhu, Prog. Opt. **45**, 119 (2003).
[10] N. Chattrapiban, E. A. Rogers, D. Cofield, W. T. Hill, III, and R. Roy, Opt. Lett. **28**, 2183 (2003).
[11] N. Chattrapiban, E. A. Rogers, I. V. Arakelyan, R. Roy, and W. T. Hill, III, J. Opt. Soc. Am. B (In Press).
[12] J. Durnin, J. Opt. Soc. Am. A **4**, 651 (1987).